Macromolecules

ARTICLE

pubs.acs.org/Macromolecules

Tailoring the Mechanical Properties of Isotactic Polypropylene by Blending Samples with Different Stereoregularity

Finizia Auriemma,* Odda Ruiz de Ballesteros,* Claudio De Rosa, and Carmine Invigorito

Dipartimento di Chimica "Paolo Corradini", Università di Napoli "Federico II", Complesso Monte S. Angelo, Via Cintia 80126 Napoli, Italy

Supporting Information

ABSTRACT: The structure and properties of some blends obtained by mixing two semicrystalline samples of isotactic polypropylene (iPP) characterized by different degree of stereoregularity have been analyzed in the whole range of composition. The two components are a highly isotactic and crystalline sample (iPP1) and a stereoirregular and less crystalline sample (iPP2), and have been synthesized using two different metallocene catalysts. The blends show separate and independent crystallization and melting of the two components, and crystallinity content decreasing almost linearly with increasing the concentration of the low stereoregular component. A continuous change of tensile properties with the composition occurs, with properties ranging from those of thermoplastic materials with high stiffness, typical of the neat iPP1, to those of high-strength elastomers, typical of neat iPP2. The mechanical properties of these blends reflect the complex lamellar morphology that develops upon crystallization, characterized by a high degree of inclusion of both components in the same stacks, with lamellae interconnected by the amorphous portions of chains of the components mixed at molecular level. Similar properties intermediate between stiff plastic materials and elastomers can also be obtained with a series of stereodefective iPP samples by tailoring the concentration of stereodefects, using different metallocene catalysts. The advantage of preparing binary blends of the two iPP samples having different concentration of stereodefects for obtaining the same properties is that only two different catalysts must be used.

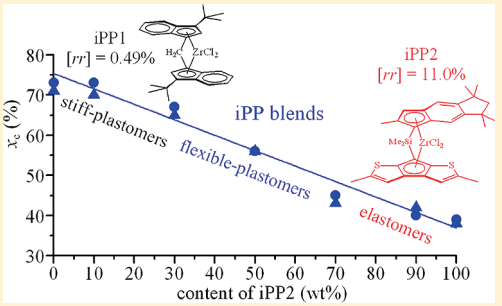

INTRODUCTION

The mixing of two vinyl polymers characterized by a different kind or degree of stereoregularity to obtain new materials with improved properties is not uncommon.[1−3] In the case of polypropylene the studies performed to date have delineated the difficulties encountered at directly probing the level of miscibility of components characterized by different kind and degree of stereoregularity in the melt and building up the phase diagram of the corresponding blends.[2,3] This is due to the similar refractive index of the two components in the melt and the scarce effect of the degree of stereoregularity on the glass transition temperature T_g, which is around 0 °C, regardless of degree of stereoregularity.[2−4] In addition, the study of the thermal behavior of these blends by standard DSC measurements is complicated by the fact that the melting point depression of a semicrystalline polymer mixed with another component is generally small.[5−7] As argued by Mandelkern,[7] this is an intrinsic property of polymer blends since the melting point depression is a colligative property and the added species are generally of high molecular mass. The blends used in this paper are a typical example of this category of mixtures.

In this paper, exploiting the ability of metallocene catalysts to synthesize polyolefins with well-defined molecular microstructures,[8−13] we have studied the structure and properties of blends obtained by mixing two samples of isotactic polypropylene of different degree of stereoregularity, which have been prepared with two different metallocene catalysts.[11] The two components of the blends have been prepared under conditions such as they present similar molecular mass, molecular mass distribution with polydispersity index around two and no detectable amount of regiodefects, the only difference being the degree of stereoregularity.[11] The ^{13}C NMR spectra of the two polymers show a random distribution of defects of stereoregularity consisting of only isolated stereoinversions (indicated as *rr* from here on, according to the NMR nomenclature).[11] In particular, we have mixed a highly stereoregular sample (iPP1) with a low concentration of *rr* stereodefects equal to 0.49 mol %, high melting temperature of ≈158 °C, and mechanical properties typical of a rigid plastomer associated with a high level of crystallinity, and a less stereoregular sample, with concentration of *rr* stereodefects of 11.0 mol %, melting in the temperature range of ≈55−88 °C and elastomeric properties associated with a low level of crystallinity.[11,12] The idea that we have pursued in the study of these blends relies in the possibility of obtaining materials with a range of properties varying from those of stiff plastomers of high rigidity, typical of iPP1, to those of more flexible materials, up to

Received: June 22, 2011
Revised: July 5, 2011
Published: July 14, 2011

Chart 1. Structures of the Zirconocene Catalysts

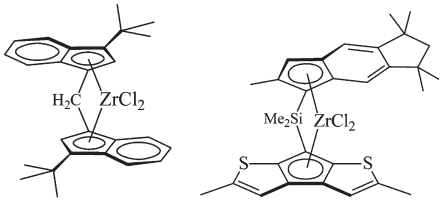

1 2

achieve elastomeric properties, typical of iPP2, by simply changing the composition of the blend.[14,15]

It is worth noting that metallocene catalysts provide a versatile route for tailoring material properties because of the large variety of accessible chemical structures of the metallocene complex precursor, each catalyst in turn producing polypropylene with different microstructures.[8−13] In particular, as shown in refs 11−13 and 16, using different catalyst systems, isotactic polypropylene samples with different microstructures, showing different crystallization behavior and different physical properties may be obtained. For instance, in the case of isotactic polypropylene stiff plastic materials, with concentration of *rr* defects up to 3−4% and melting temperatures of 130−160 °C, highly flexible materials, with *rr* content of 5−6% and melting temperatures around 115−120 °C, and high-strength elastomers, with [*rr*] = 7−11% and melting temperatures in the range 80−110 °C, can be produced.[11,12] Within this framework we have explored the possibility of obtaining materials showing properties that gradually vary from those of stiff to flexible and finally to elastomeric materials, depending on blend composition, making use of only two catalysts for the synthesis of the iPP components, instead of using different catalysts for each desired property.

Of course the possibility of tailoring material properties by blending two semicrystalline polymers is critically dependent on the degree of mixing at molecular level of the two components in the melt, and on the number of phases and interphases and the overall morphology that develops upon crystallization.[6]

Recently, using a theoretical approach for analysis of small-angle X-ray scattering (SAXS) data from semicrystalline blends, a unified vision of the complex morphology at nanometer length scale of the blends iPP1/iPP2 has been obtained.[15] Our theoretical approach allows overcoming some limitations of more classic methods of analysis of SAXS data, in cases of blends of semicrystalline/semicrystalline polymers crystallized from the melt in conditions far from thermodynamic equilibrium. We have shown not only that lack of definite correlation peaks in the SAXS profiles associated with the presence of large amount of diffuse scattering shown by some blends does not necessarily correspond to the lack of lamellar morphology but also that these featureless SAXS patterns may also originate from lamellar stacks with the lamellae of the two components randomly mixed within the same array, stacked with faults. In particular, it has been demonstrated that the nanostructural organization of the blends iPP1/iPP2 depends on the composition. In all cases mixed lamellar stacks are formed. In the case of blends rich in the highly stereoregular and high temperature crystallizing (HTC) component iPP1, a high degree of inclusion of lamellae of the second less stereoregular component is achieved, up to reach the maximum degree of inclusion in the blends with ≈30 wt % iPP2. In the case of blends rich in the less stereoregular and low temperature crystallizing (LTC) component iPP2, at least two families of lamellar stacks are formed: a family rich in the component iPP1, which forms at high temperatures, achieving the maximum degree of inclusion of lamellae of the component iPP2, and a second family that forms at lower temperatures, including the excess of the component iPP2 and eventually the lamellae of iPP1 not comprised in the first family.[15] Formation of mixed lamellar stacks in these systems provides clear evidence that the two components are miscible in the melt state.

Table 1. Polymerization Temperatures (T_p), Viscosity Average Molecular Masses (M_v), Content of Triad Stereosequences, and Melting Temperatures (T_m) of the iPP Samples Prepared with Catalysts of Chart 1

sample	T_p (°C)	catalyst	M_v[a]	[*mm*] (%)[b]	[*mr*] (%)[b]	[*rr*] (%)[b]	T_m (°C)[c]
iPP1	50	**1**/MAO	195 700	98.54	0.98	0.49	158
iPP2	50	**2**/MAO	162 000	67.0	22.0	11.0	55−88

[a] Viscosity average molecular mass, derived from the intrinsic viscosities values through the equation $[\eta] = K(M_v)^{\alpha}$, with $K = 1.93 \times 10^{-4}$ and $\alpha = 0.74$.[17] [b] From ^{13}C NMR analysis. [c] Measured from DSC scans at heating rate of 10 °C/min of melt crystallized compression-molded samples.

In this paper the structure, and thermal and mechanical properties of binary blends of iPP1 and iPP2 are analyzed in the framework of all structural information gained at nanometer length scale in ref 15, with the aim of establishing precise correlations between the microstructure of the chains of the components, the structural organization of crystalline and amorphous phases and the mechanical properties. This analysis is accomplished by performing a direct comparison of the properties of iPP1/iPP2 blends with the properties of a parent series of stereodefective iPP samples prepared using different metallocene catalysts, characterized by molecular mass similar to those of iPP1 and iPP2 components, the absence of regiodefects, and concentration of *rr* stereodefects similar to the average concentration of defects in the iPP1/iPP2 mixtures.[11,12]

EXPERIMENTAL SECTION

Materials. The samples used for preparation of blends have been synthesized with the catalysts **1** and **2** of Chart 1. The C_2-symmetric *ansa*-zirconocene catalyst **1** is fully regioselective and produces iPP samples of high stereoregularity, molecular mass and melting temperature (sample iPP1, Table 1).[11b] The C_1-symmetric zirconocene catalyst **2** of Chart 1 produces fully regioregular iPP samples of low stereoregularity and melting temperature (sample iPP2 of Table 1).[11c] Both catalysts **1** and **2** are activated with methylalumoxane (MAO).

The properties of the blends iPP1/iPP2 in the whole range of composition have been compared with those of a parent series of stereodefective iPP samples prepared using different metallocene catalysts listed in Table S1, Supporting Information. These samples are characterized by similar molecular mass, absence of regiodefects, and concentration of *rr* stereodefects intermediate between those of iPP1 and iPP2.

Preparation of Blends. The blends have been prepared by dissolving the samples iPP1 and iPP2 in the appropriate weight ratio in refluxing xylene (bp 140 °C) for 1 h, up to obtain homogeneous solutions. The components were then precipitated from hot solutions using an excess (3:1) of cold methanol, and the so obtained powders were filtered and dried under vacuum at 60 °C for 1 day. About 1 wt % of BHT (2,6-di-*tert*-butyl-4-methylphenol) was added in the methanol as an antioxidant. The weight loss of dried samples has been checked to be in all cases less than 1%, indicating that the dissolution and successive

precipitation of the two components was complete. Five blends of composition 10/90, 30/70, 50/50, 70/30, 90/10 wt %/wt % have been prepared. The different blend samples are designated as iPP1-*x*/iPP2-*y*, with *x* and *y* the weight percent of iPP1 and iPP2, respectively.

Compression molded films of the iPP blends have been prepared by melting the dry-precipitated powders at 180 °C for 10 min under a press at very low pressure, to avoid preferred orientation in the film, and cooling to room temperature. Oriented fibers of the iPP blends have been then obtained by stretching compression molded films at room temperature and at a drawing rate of 10 mm/min.

X-ray Diffraction. The X-ray diffraction patterns have been obtained with Ni filtered Cu Kα radiation. The diffraction powder profiles of unoriented samples have been obtained with an automatic Philips diffractometer. The indices of crystallinity (x_c) have been evaluated from the X-ray powder diffraction profiles by the ratio between the crystalline diffraction area and the total area of the diffraction profile. The crystalline diffraction area has been obtained from the total area of the diffraction profile by subtracting the amorphous halo. The amorphous halo has been obtained from the X-ray diffraction profile of an atactic polypropylene, then it was scaled and subtracted to the X-ray diffraction profiles of the samples.

The X-ray fiber diffraction patterns have been recorded on BAS-MS imaging plate (FUJIFILM) using a cylindrical camera (radius = 57.3 mm) and processed with the digital imaging reader FUJIBAS 1800. The X-ray fiber diffraction patterns have been recorded on the oriented fibers soon after the stretching, keeping the fiber under tension (exposition time 2 h), and on the relaxed specimens after removing the tension.

Differential Scanning Calorimetry (DSC). The thermal analysis has been performed with a Mettler-DSC30/2285 apparatus, equipped with a liquid nitrogen cooling system for measurements at low temperature. The scans have been recorded in flowing nitrogen atmosphere at a scan rate of 10 °C/min.

Mechanical Tests. The mechanical tests have been performed at room temperature on unoriented compression molded films and oriented fibers of the iPP blends with a miniature mechanical material tester (MINIMAT, by Rheometrics Scientific), following the standard test method for tensile properties of thin plastic sheeting ASTM D882−83. The mechanical tests have been first performed on unstretched compression molded films. Rectangular specimens 10 mm long, 2−4 mm width and 0.3−0.5 mm thick were stretched up to the break or up to a given strain $\varepsilon = 100 \times (L_f - L_0)/L_0$, with L_f and L_0 the final and initial lengths of the specimen, respectively. Two benchmarks were placed on the test specimens and used to measure elongation. Similar tests have been then performed on oriented stress-relaxed fibers. The stress-relaxed fiber specimens have been prepared by stretching unoriented compression molded films of initial length L_0 up to $L_f = 3.5L_0$ ($\varepsilon = 250\%$) and $L_f = 6L_0$ ($\varepsilon = 500\%$), keeping the fibers under tension for 10 min, then removing the tension allowing complete relaxation of the specimens.

In order to quantify the elasticity of the iPP blends values of tension set and elastic recovery at a given strain ε ($t_s(\varepsilon)$ and $r(\varepsilon)$, respectively) have been measured according to the standard test method for rubber properties in tension ASTM D412−87. Compression-molded specimens of initial length L_0 were stretched at room temperature up to a length L_f ($\varepsilon = 100 \times (L_f - L_0)/L_0$), held at this deformation for 10 min, then the tension was removed and the length of the relaxed specimens L_r was measured after 10 min. The values of tension set and elastic recovery were calculated as $t_s(\varepsilon) = 100 \times (L_r - L_0)/L_0$ and $r(\varepsilon) = 100 \times (L_f - L_r)/L_r$, respectively. Values of the tension set and elastic recovery have also been measured on unoriented compression molded samples after breaking (t_b and r_b, respectively), following the procedure described in the ASTM D 412−87. Specimens of initial length L_0 have been stretched up to the break. Ten minutes after breaking, the two pieces of the sample have been fit carefully together so that they are in contact over the full area of the break and the final total length L_r of the specimen has been obtained by measuring the distance between the two benchmarks. The tension set and elastic recovery at break have been calculated as $t_b = 100 \times (L_r - L_0)/L_0$ and $r_b = 100 \times (L_f - L_r)/L_r$, respectively.

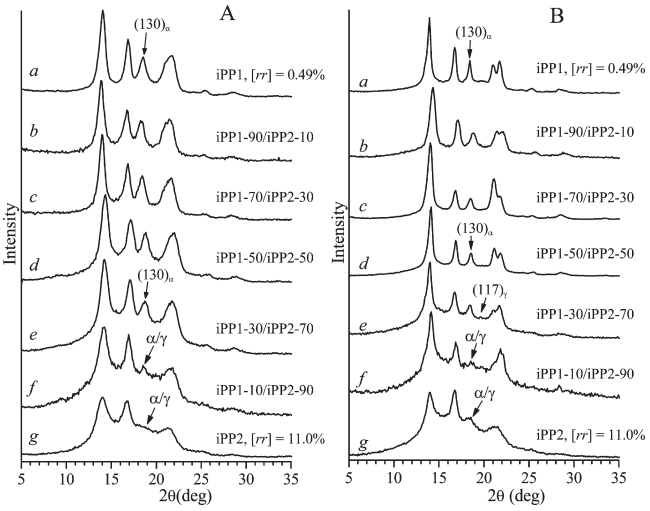

Figure 1. X-ray diffraction profiles of iPP1 (a) and iPP2 (g) neat components and of blends iPP1/iPP2 (b−f) of indicated compositions for solution precipitated samples (A) and melt crystallized films (B). The $(130)_\alpha$ reflection of α form,[23] and $(117)_\gamma$ reflection of γ form,[24] at $2\theta \approx 18$ and 20°, respectively, are indicated by arrows. For curves f and g, these reflections merge into a single broad peak, due to crystallization in disordered modifications intermediate between α and γ forms (α/γ disorder).[21b,25]

Mechanical cycles of stretching and relaxation have been performed at room temperature on the stress-relaxed fibers of the iPP blends and the corresponding hysteresis has been recorded. In these cycles, the stress-relaxed fibers with initial length L_r were stretched again up to the final length $L_f = 3.5L_0$ ($\varepsilon = 250\%$) or $L_f = 6L_0$ ($\varepsilon = 500\%$) and then relaxed at controlled rate. After each cycle the values of tension set have been measured.

In the mechanical tests the ratio between the drawing rate and the initial length was fixed equal to 0.1 mm/(mm × min) for the measurement of Young's modulus and 10 mm/(mm × min) for the measurement of stress−strain curves and the determination of the other mechanical properties (stress and strain at break and tension set). The reported stress−strain curves and the values of the mechanical properties are averaged over at least five independent experiments.

RESULTS AND DISCUSSIONS

Polymorphic Behavior. It is well-known that metallocene-made iPP samples, characterized by chains including different types of microstructural defects (stereodefects, or regiodefects), generally crystallize as mixtures of α and γ forms, and the relative amount of the two polymorphs depends on the crystallization temperature and the content of defects.[11−13,18−20] The formation of γ form is favored by the presence of stereodefects (mainly isolated *rr* triads)[11,12,18,21] and/or regiodefects (mainly 2,1 and 3,1 insertions)[13b,18,20] and also by the presence of constitutional defects, like comonomeric units.[19,20,22]

The X-ray powder diffraction profiles of as-polymerized samples of the neat iPP1 and iPP2 and as-prepared samples of the blends iPP1/iPP2, after precipitation from solution and drying, are reported in Figure 1A. They are compared with the X-ray powder diffraction patterns of compression molded films of the samples obtained by crystallization from the melt to room

temperature (Figure 1B). Similar profiles in the case of melt pressed films have been already discussed in ref.[15]

In both cases the highly isotactic sample iPP1 ([*rr*] = 0.49%) crystallizes in the α form, as indicated by the presence of the $(130)_\alpha$ reflection at $2\theta = 18.6°$ of the α form[23] and the absence of the $(117)_\gamma$ reflection at $2\theta = 20.1°$ of the γ form[24] in the X-ray diffraction profile a of Figure 1.[11] The less stereoregular sample iPP2 ([*rr*] = 11.0%), instead, crystallizes from solution in

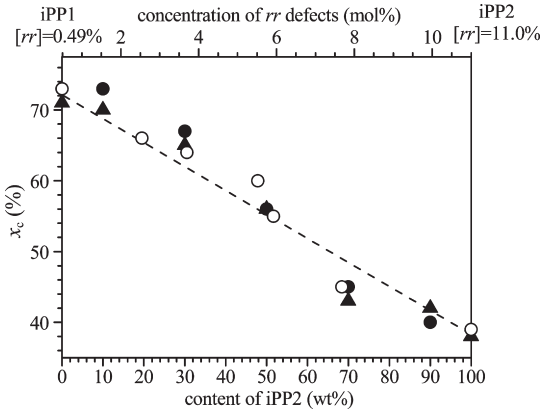

Figure 2. Content of crystallinity of blends iPP1/iPP2 for the solution precipitated (▲) and melt-crystallized samples (●) as a function of blend composition (lower horizontal scale) and the average concentration of *rr* stereodefects of an equivalent single component system ([*rr*(eq)]) (upper horizontal scale). The content of crystallinity of melt-crystallized samples of stereodefective iPPs (○), having concentration of *rr* stereodefects intermediate between those of samples iPP1 and iPP2 is also reported as a function of *rr* concentration (upper horizontal scale).[12] The average concentration of *rr* stereodefects of blends has been calculated as $[rr(eq)] = (1 - x)0.49 + x11.0$, with x the weight fraction of the iPP2 component in the blend.

disordered modification of the γ form intermediate between α and γ forms (α/γ disordered modifications),[11,21b,25] as indicated by the low intensity of both $(130)_\alpha$ and $(117)_\gamma$ reflections in the diffraction profile g of Figure 1.

In both as-prepared and melt-crystallized samples, all blends crystallize as a mixture of crystals of α form, due to the component iPP1, and of α/γ disordered modifications, due to the component iPP2, even though the diffraction profiles of blends for each composition is dominated by the Bragg peaks of the most crystalline component iPP1, down to iPP1 concentrations of 30 wt %. In fact, blends with content of iPP1 in the range 90 - 30 wt % basically crystallize in the α form, as indicated by the presence of the $(130)_\alpha$ reflection at $2\theta = 18.6°$ in profiles b−e of Figure 1A,B. For concentrations of iPP1 lower than 30 wt % the blends crystallize basically in α/γ disordered modifications, in mixture with low amount of α form, as evident by the decrease of the intensity of the $(130)_\alpha$ reflection in the profiles e and f of Figure 1A,B. At 30 wt % content of iPP1 a faint $(117)_\gamma$ reflection of γ form at $2\theta = 20.1°$ is present in curve e of Figure 1B, and only for the blend with 10 wt % iPP1 (curve f of Figure 1) the intensity of the $(130)_\alpha$ reflection of α form becomes less evident, and the formation of α/γ disordered modifications, as in the case of neat iPP2, mixed with a low amount of crystals of α form, is apparent.

The content of crystallinity derived from the X-ray diffraction profiles of Figures 1 is reported in Figure 2 as a function of blend composition. In the same figure the crystallinity content of stereodefective iPP samples having stereoregularity intermediate between those of the samples iPP1 and iPP2 is also reported for comparison, as a function of the concentration of *rr* sterodefects.[11,12] To this aim, we have associated with each sample of blend the parameter [*rr*(eq)] that represents the average concentration of *rr* stereodefects in the blend, given by $rr(eq) = (1 - x)0.49 + x11.0$, with 0.49 and 11.0 being the concentration of *rr* sterodefects in iPP1 and iPP2, respectively, and x the weight fraction of

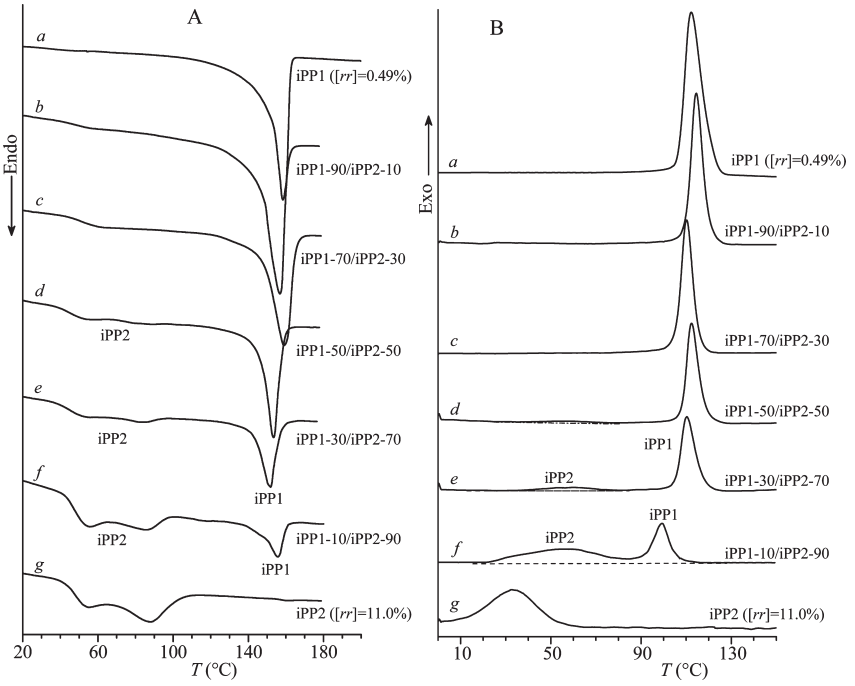

Figure 3. DSC heating (A) and cooling (B) scans, recorded at 10 °C/min, of melt-crystallized compression-molded samples of the blends iPP1/iPP2 of the indicated composition. The DSC curves recorded at 10 °C/min of compression-molded samples of the highly stereoregular iPP1 (a) and less stereoregular iPP2 (g) neat components are also reported.

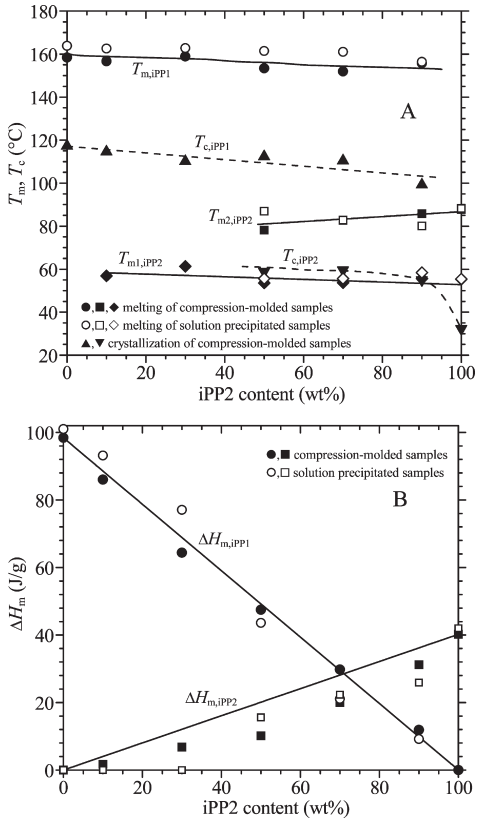

Figure 4. Values of melting (●, ○, ■, □, ♦, ◊) and crystallization (▲, ▼) temperatures (A) and melting enthalpy (●, ○, ■, □) (B) of iPP1 and iPP2 components in the blends iPP1/iPP2 and neat samples, for compression-molded films (full symbols) and solution precipitated powders after drying (open symbols), measured from the DSC curves of Figures 3 and S2B (Supporting Information), respectively, as a function of blend composition.[15]

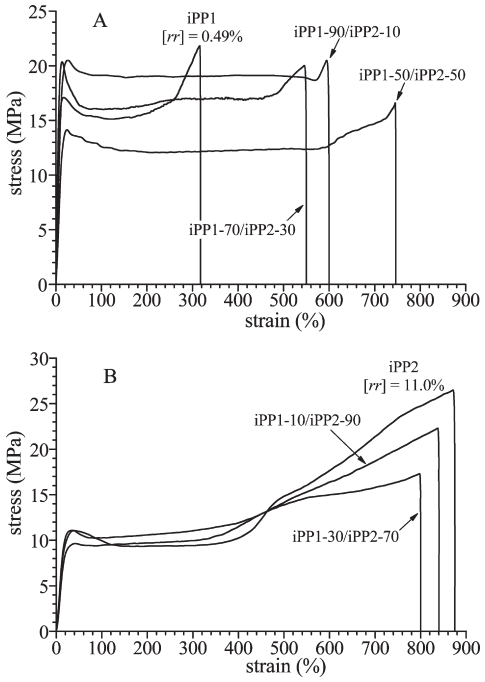

Figure 5. Stress−strain curves recorded at room temperature of unoriented compression molded films of the blends iPP1/iPP2 and of the neat components iPP1 and iPP2.

the iPP2 component in the blend. The value of the parameter [*rr*(eq)] corresponds to the concentration of isolated *rr* triads of an equivalent stereodefective iPP sample, obtained as if the *rr* defects of iPP1 and iPP2 components in a blend were uniformly distributed over all the chains.

The crystallinity of blends iPP1/iPP2 decreases almost linearly with increasing the content of the low stereoregular component iPP2 (full symbols in Figure 2) suggesting that the crystallization ability of each of the two components is not greatly influenced by the presence of the other component, also in agreement with DSC results (vide infra). Furthermore, the decrease of crystallinity content follows the same trend as observed in the case of stereodefective iPP samples with increasing the amount of *rr* stereodefects (open symbols in Figure 2). This indicates that the influence of the composition of blends on the crystallinity is similar to that produced by the increase of concentration of *rr* stereodefects in melt-crystallized samples of stereodefective iPP samples.

Thermal Analysis. The DSC heating curves of melt-crystallized compression-molded samples and the cooling scans from the melt of the neat components iPP1 and iPP2 and of iPP1/iPP2 blends, recorded at 10 °C/min, are reported in Figure 3, parts A and B, respectively. Similar data have been already presented and discussed in ref.[15] The blends iPP1/iPP2 show, regardless of composition, separate and sequential crystallization and melting of the two components, with the highly stereoregular component iPP1 crystallizing and melting at high temperatures and the low stereoregular component iPP2 crystallizing and melting at lower temperatures. In particular, the melting and crystallization of the component iPP1 occur at temperatures close to the temperatures of melting and crystallization of the neat sample iPP1, equal to ≈154 and ≈112 °C, respectively. For the low stereoregular component iPP2, the double melting behavior in the range 50−90 °C of neat iPP2 is retained also in the blends. The major differences occur for the crystallization temperature of the component iPP2, which, in the blends is at ≈55−60 °C, that is, ≈ 30 °C higher than that of neat iPP2, equal to 32 °C. The increase of crystallization temperature of iPP2 in the blends has been attributed to the nucleating effect of the already formed crystals of the HTC component iPP1 on the LTC component iPP2.[15]

As show in the Supporting Information, the melting behavior of solution precipitated blends, after drying (Figure S2B, Supporting Information), is similar to that of melt-crystallized compression-molded films (Figures 3A and S2A (Supporting Information)), regardless of the composition. This result indicates that a good degree of blending is achieved already in the preparation step from solution, and reflects the good degree of compatibility of the chains of iPP1 and iPP2 constituents, in the melt, in the amorphous phase, as well as in solution in a common solvent.

The values of melting and crystallization temperatures of the components iPP1 and iPP2 in the blends and of pure components obtained from DSC scans of compression-molded films and the values of melting temperature of solution precipitated powders are reported in Figure 4A as a function of the blend composition. The decrease of melting temperature of both components and crystallization temperature of the highly stereoregular iPP1 in the blends is small, regardless of the preparation method. The small melting point depression of our blends has

Table 2. Values of Young's Modulus (E), Stress and Strain at Yield (σ_y and ε_y) and at Break (σ_b and ε_b), Tension Set and Elastic Recovery at Break (t_b and r_b), and Crystallinity Content (x_c) of Unoriented Compression Molded Films of the Blends iPP1/iPP2 and of the Neat Components iPP1 and iPP2

sample	$E \times 10^{-2}$ (MPa)	σ_y (MPa)	ε_y (%)	σ_b (MPa)	$\varepsilon_b \times 10^{-2}$ (%)	$t_b \times 10^{-2}$ (%)	$r_b \times 10^{-2}$ (%)	x_c (%)[a]
iPP1	2.7 ± 0.3	17 ± 2	16 ± 2	22 ± 3	3.1 ± 0.5	3.1 ± 0.5	0	73
iPP1−90/iPP2−10	2.3 ± 0.3	21 ± 3	20 ± 3	21 ± 3	6.0 ± 0.50	5.7 ± 0.5	0.08	73
iPP1−70/iPP2−30	2.1 ± 0.5	20 ± 1	15 ± 5	20 ± 3	6 ± 1	4.0 ± 0.3	0.2	67
iPP1−50/iPP2−50	1.3 ± 0.1	14 ± 2	21 ± 3	17 ± 4	7.5 ± 0.5	3.0 ± 0.5	1.1	56
iPP1−30/iPP2−70	0.62 ± 0.01	11 ± 2	29 ± 2	17 ± 2	8.0 ± 0.8	2.5 ± 0.3	1.5	43
iPP1−10/iPP2−90	0.55 ± 0.08	10 ± 1	38 ± 6	22 ± 4	9 ± 1	1.7 ± 0.4	2.5	40
iPP2	0.48 ± 0.01	11 ± 1	35 ± 4	26 ± 6	9 ± 1	1.6 ± 0.4	2.9	39

[a] From X-ray diffraction analysis (Figure 2).

been explained by the fact that the values of lamellar thickness achieved upon crystallization by the components iPP1 and iPP2 in the blends are similar to those of pure components, crystallized in similar conditions.[15] Such morphological features are associated with thermodynamic considerations. In fact since iPP1 and iPP2 in the melt and amorphous state are miscible, owing to the chemical similarity of the two components, their reciprocal interactions are so weak that the chemical potentials of the chains in the blends are not greatly altered with respect to those of neat components.[1,6,7]

The experimental values of the melting enthalpy of compression-molded films obtained from DSC scans of Figure 3A and those of samples precipitated from solution as powders measured from DSC curves of Figure S2A (Supporting Information) are compared in Figure 4B with those calculated assuming complete crystallization of the two components. The calculated values have been obtained by multiplying the value of melting enthalpy of neat iPP1 (98.7 J/g) and iPP2 (40.2 J/g) by the corresponding weight fraction in the blend. It is apparent that for iPP1 the values of $\Delta H_{m,iPP1}$ in the blends are nearly identical to those calculated. For the low stereoregular component iPP2, instead, the values of $\Delta H_{m,iPP2}$ are slightly lower than those calculated. This indicates that, regardless of thermal history of our blends, whereas the crystallization from the homogeneous melt of the highly stereoregular component iPP1 is undisturbed as in the neat sample, for the low stereoregular iPP2 component the constrained crystallization within the preformed lamellar crystals of the component iPP1 in somehow precludes the full crystallization of iPP2.

Mechanical Properties. The stress−strain curves of unoriented compression-molded films of the blends iPP1/iPP2 and of the neat components iPP1 and iPP2 are reported in Figure 5. The values of Young's modulus (E), stress and strain at yield point (σ_y and ε_y) and at break (σ_b and ε_b), tension set and elastic recovery at break (t_b and r_b) are reported in Table 2.

The highly stereoregular and crystalline sample iPP1 behaves as stiff material, whereas the stereodefective sample iPP2 shows properties of a high-strength elastomer (Figure 5 and Table 2).[11,12] The blends iPP1/iPP2 show mechanical behavior intermediate between those of the neat components iPP1 and iPP2. In particular, blends having iPP1 content higher than 50 wt % are stiff materials, with high values of Young's modulus (200−300 MPa) and stress at yield (20−25 MPa), due to the high crystallinity (Figure 2). The addition of only 10 wt % of the stereoirregular component iPP2, however, produces enhancement of ductility and flexibility (ε_b = 600%), but does not induce elastomeric properties, the value of residual deformation after breaking t_b of 570% being similar to the deformation at break (Figure 5A and Table 2).

With increasing content of iPP2 in the blend, a further decrease of Young's modulus and increase of ductility are observed, associated with the development of elastomeric properties, as indicated by the decrease of the values of tension set after breaking (Table 2). For instance, the blend iPP1−50/iPP2−50 behaves as a flexible thermoplastic material, with values of Young's modulus and stress at yield intermediate between those of iPP1 and iPP2 and with partial elastic recovery after breaking (Figure 5A and Table 2).

The elastomeric properties improve with further increase of the concentration of the stereoirregular component iPP2. The blends iPP1/iPP2 with iPP2 content higher than 50 wt %, indeed, behave as a high-strength elastomeric material, with low values of Young's modulus and stress at yield, high values of strain at break (ε_b = 800−850%) and high tensile strength (σ_b = 17−22 MPa), due to the strong strain hardening at high deformations, associated with good elastomeric properties (Figure 5B and Table 2).

The values of tensile parameters of the blends iPP1/iPP2, evaluated from the stress−strain curves of Figure 5, are reported in Figure 6 as a function of the blend composition. The values of the tensile parameters of stereodefective iPP samples, having concentrations of *rr* defects intermediate between those of the samples iPP1 and iPP2, are also reported in Figure 6 as a function of *rr* content.[11,12] This allows making a direct comparison between the mechanical properties of blends and those of an equivalent single component system having a degree of stereoregularity *rr*(eq) given by the average concentration of *rr* stereodefects in the blends.

It is apparent from Figure 6 that the tensile behavior of the blends iPP1/iPP2 is similar to that of the stereodefective iPPs, especially at low deformations. In fact, the decrease of the Young's modulus (Figure 6A) and stress at yield (Figure 6B) and the increase of the deformation at break (Figure 6C) observed in stereodefective iPP samples with increasing concentration of *rr* defects,[11,12] are similar to the trends observed in the blends iPP1/iPP2 with increasing the content of the stereoirregular component iPP2. Moreover, the values of stress at break (Figure 6B) strongly increase for high concentration of stereodefects in the iPP samples, or of the stereoirregular component iPP2 in the blends iPP1/iPP2, due to the strain hardening occurring at high deformations for less crystalline and more defective samples.

The continuous change of the tensile properties with the composition of the blends iPP1/iPP2 is in agreement with the gradual decrease of crystallinity (Figure 2), which accounts for the decrease of Young's modulus (Figure 6A) and the increase of

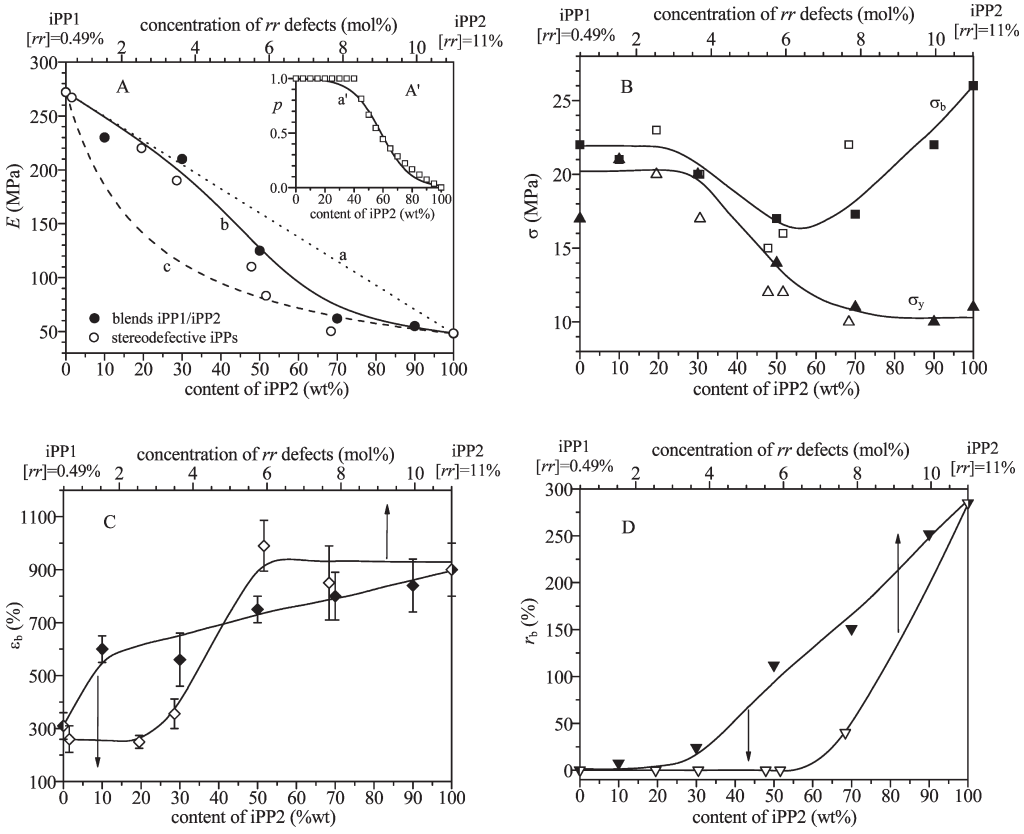

Figure 6. Values of Young's modulus E (●, ○) (A), stress at break σ_b (■, □) and stress at yield σ_y (▲, Δ) (B), strain at break ε_b (♦, ◊) (C) and elastic recovery at break r_b (▼, ▽) (D) of melt crystallized samples of the blends iPP1/iPP2 (full symbols) as a function of the blend composition (lower horizontal scale) and the average concentration *rr*(eq) of stereodefects of an equivalent single component system (upper horizontal scale), and of stereodefective iPP samples (open symbols) as a function of the *rr* concentration.[11,12] In part A, curves a and c have been calculated using the mechanics of material models in the limiting cases of isostrain (Scheme 1A, eq 1) and isostress models (Scheme 1C, eq 2), respectively. Curve b has been calculated with the eq 3 according to the combination model B of Scheme 1 to fit the experimental data. Inset A′: values of p calculated for ϕ_{max} = 0.4 using eq 4 (□) and continuous curve obtained by modeling the value of p with a sigmoid function (curve a′).

ductility (Figure 6C) with increasing the concentration of the stereoirregular component iPP2. It is worth noting that, contrary to the stereodefective iPP samples that need incorporation of at least 5−6 mol % of *rr* stereodefects to obtain a significant increase of ductility and flexibility,[11,12] for the blends even a small amount (≈10 wt %) of the stereoirregular component iPP2 induces a considerable increase of the deformation at break (Figure 6C).

In Figure 6A, the experimental values of the Young's modulus of the blends are compared with the calculated values (dotted and dashed lines), evaluated by the weighted average (eq 1) and the weighted harmonic average (eq 2), respectively, of the Young's moduli of the neat components iPP1 and iPP2, weighed by the corresponding volume fractions ϕ and $1 - \phi$ of the components iPP2 and iPP1, respectively:

$$E_c = (1 - \phi)E_{iPP1} + \phi E_{iPP2} \quad (1)$$

$$E_c = [(1 - \phi)/E_{iPP1} + \phi/E_{iPP2}]^{-1} \quad (2)$$

It may be shown that eq 1 corresponds to a model where the two components iPP1 and iPP2 act as two elements (modulus E_{iPP1} and E_{iPP2}) working in parallel (Scheme 1A) so that they experience the same level of strain (*isostrain* model), whereas eq 2 corresponds to a model where the two components iPP1 and iPP2 act as two elements working in series (Scheme 1C) so that they experience the same level of stress (*isostress* model).[26] The *isostrain* model represents an upper bound model, where the predicted modulus is the highest achievable, whereas the *isostress* model is a lower bound model, yielding the lowest modulus the material may have.[26] At low deformations, samples of blends iPP1/iPP2 with high content of the highly stereoregular and crystalline component iPP1 behave as stiff materials (Figure 5 and Table 2) and the dependence of Young's modulus on the blend composition is well described by the upper bound *isostrain* model (Figure 6A, dotted line). Samples of blends iPP1/iPP2 with high content of the stereoirregular component iPP2, instead, have elastomeric properties (Figure 5 and Table 2) and exhibit lower bound *isostress* behavior (Figure 6A, dashed line). The tensile behavior of the blend iPP1−50/iPP2−50 is intermediate between that of plastic and rubbery materials and the values of Young's modulus are intermediate between the values predicted by the *isostress* and *isostrain* models (Figure 6A).

It is worth noting that, by exploiting the concept of phase continuity in heterogeneous systems as proposed by Kolarik in ref 27, these models may be used to a first approximation to describe the mechanical behavior of heterogeneous systems characterized by phase continuity of both components in the case of isostrain model; i.e., each phase is continuous in the direction parallel to the direction of the applied tensile stress, by

Scheme 1. Mechanics of Material Models for the Blends iPP1/iPP2 with Volume Fraction ϕ of the Rubbery Component iPP2 in the Limiting Case of Isostrain (A) and Isostress Models (C) and Combination Model (B)[a]

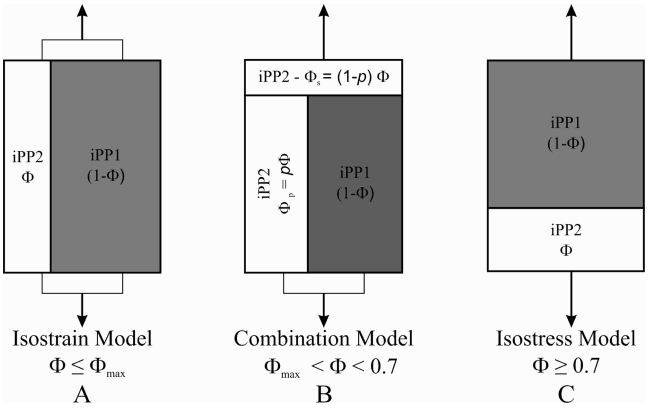

[a] In the combination model (B) a fraction $\phi_p = p\phi$ of the component iPP2 is included within the lamellar stacks of the highly stereoregular component iPP1 crystallizing at high temperatures, and a fraction $\phi_s = \phi(1 - p)$ of iPP2 is rejected outside these mixed lamellar stacks. This model is idealized as if the entire amount of the component iPP1 (volume fraction $1 - \phi$) were working in parallel with a fraction ϕ_p of the component iPP2, the remaining fraction ϕ_s of iPP2 that is rejected outside these mixed lamellar stacks is assumed as working in series with the first two phases.

no phase continuity of constituents for the isostress model, i.e., lack of continuity of the phases in the direction parallel to the direction of the applied tensile stress, due for instance to an insufficient degree of connectivity between the phases. The fact that the isostrain and isostress models work quite well also for our blends, may be envisaged in the peculiar morphology of the blends iPP1/iPP2 at nanometer length scale. In fact, as demonstrated in ref 15, blends iPP1/iPP2 have a complex morphology derived from the tight intermingling of the chains of the two components in the melt, and tendency of iPP1 and iPP2 to crystallize separately, forming mixed lamellar stacks, where the lamellae of the two components are connected by an entangled amorphous network constituted by the chains of the two components mixed at molecular level. In particular, as shown in ref 15, in the case of blends rich in the high temperature crystallizing component iPP1, the lamellae of the second less stereoregular component iPP2 are entirely included in the lamellar stacks of iPP1, up to reach a maximum degree of inclusion of iPP2 corresponding to $\phi_{max} \approx 0.3-0.4$.[28] In these blends, the two constituents form two cocontinuous phases, the phase continuity of the two components being ensured by the miscibility at molecular level of the chains of iPP1 and iPP2 in the amorphous regions placed in between the lamellae. Therefore, blends with iPP2 content less than 30% behave at low deformation namely opposing the high rigidity of the well ordered crystals of α form of the component iPP1, coupled with the high flexibility of the disordered crystals of the low stereoregular component iPP2. This gives rise to stiff materials which substantially exhibit the upper bound isostrain behavior, where iPP1 and iPP2 sense the applied stress as working in parallel.[27] In other terms, phase continuity in blends with iPP2 content $\phi \leq \phi_{max}$ is ensured by the formation of a continuous network that is guaranteed by the miscibility of the components in the melt and in the amorphous phase and in which the well interlocked crystalline lamellae of the two components form junctions of nanometer size.

In the case of blends rich in the less stereoregular component iPP2, at least two families of lamellar stacks are formed. A family rich in iPP1, which forms at high temperatures, achieving the maximum degree of inclusion of lamellae of the component iPP2 equal to ϕ_{max}, and a second family of lamellar stacks that forms at lower temperatures, including the excess of the component iPP2 and eventually the iPP1 lamellae not included in the first family. Therefore, for blends with iPP2 content ϕ higher than ϕ_{max}, a fraction ϕ_p of the rubbery component iPP2 is included in the lamellar stacks of the HTC component iPP1, and a fraction ϕ_s of iPP2 is rejected outside these lamellar stacks that form at high temperatures (with $\phi = \phi_p + \phi_s$), where ϕ_p may be calculated considering that the maximum concentration of iPP2 within these stacks corresponds to $\phi_{max}/(1-\phi_{max})$, so that $\phi_p = (1 - \phi)[\phi_{max}/(1 - \phi_{max})]$. As a consequence, with increasing the iPP2 concentration, the amount of iPP2 included within the lamellar stacks of the HTC component iPP1 decreases, whereas the amount of the component iPP2 that is excluded, ϕ_s, increases. Applying the concept of phase continuity to these blends,[27] we have observed that a good degree of continuity occurs only between the amount $(1 - \phi)$ of the component iPP1 and the fraction ϕ_p of the component iPP2 involved in the mixed lamellar stacks, the remaining fraction of iPP2, ϕ_s, being scarcely "connected" to the rest of the material. The gradual decrease of the degree of continuity of iPP1 and iPP2 constituents with the concentration of iPP2, in turn, results, for the blends with content of the HTC component iPP1 less than ≈30%, in no effective phase continuity of constituents, so that these blends behave as soft materials exhibiting mechanical behavior at low deformation more close to the lower bound isostress model, where iPP1 and iPP2 sense the applied stress as working in series.[27]

In order to better account for the crossover from the upper bound isostrain behavior to the lower bound isostress behavior of our blends with increasing the iPP2 content we have used a combination model intermediate between the isostress and isostrain models,[26c] in the assumption of a continuous change of phase continuity of the components with composition. As an example, a good fit of the experimental values of the Young modulus of our blends could be obtained through the use of the combination model illustrated in the Scheme 1B, where the entire amount of the HTC component (volume fraction $1 - \phi$) is assumed as working in parallel only with the portion of the rubbery component iPP2 included within the mixed lamellar stacks that are formed at high temperature (volume fraction $\phi_p = p\phi$), whereas the remaining amount, which is rejected outside these mixed lamellar stacks, (volume fraction $\phi_s = \phi(1 - p)$), is assumed as working in series with the first two phases. Therefore, the parameter p may be regarded as a sort of partition coefficient of the low stereoregular component in two kinds of regions, the regions that are well interconnected with the component iPP1, and the nonconnected regions. As long as the iPP2 content is below ϕ_{max} the rubbery component is entirely included within the lamellar stacks of the HTC component and $p = 1$, whereas for blends with iPP2 content $\phi > \phi_{max}$ the value of p decreases with ϕ according to the equation $p = [\phi_{max}/(1 - \phi_{max})][(1 - \phi)/\phi]$ up to reach the value of 0 for $\phi = 1$.

The constitutive equation that relates the Young modulus E_c of blends to those of the components iPP1 and iPP2 in the case of

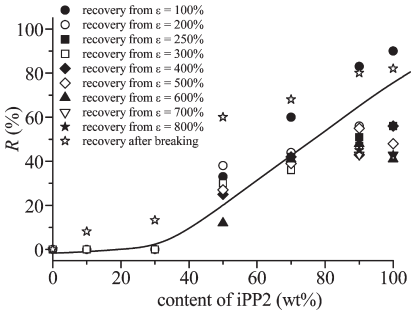

Figure 7. Values of percentage of strain which is recovered (R) by stretching unoriented compression molded films of the blends iPP1/iPP2 up to a maximum deformation ε upon release of the tension, and after breaking, as a function of blend composition.

the combination model of Scheme 1B is given by:[26c]

$$\frac{1}{E_c} = \frac{(1-p)\phi}{E_{iPP2}} + \frac{[1-\phi(1-p)]^2}{p\phi E_{iPP2} + (1-\phi)E_{iPP1}} \quad (3)$$

with $p = 1$ *for* $\phi \leq \phi_{max}$ *and*

$$p = \frac{\phi_{max}}{1-\phi_{max}}\frac{1-\phi}{\phi} \text{ for } \phi \geq \phi_{max} \quad (4)$$

In agreement with the results of ref 15, the values of p to be introduced in the eq 3 have been calculated using the eq 4 by varying the value of ϕ_{max} in the range of 0.3−0.4, close to the value of the maximum amount of rubbery component that is included within the mixed lamellar stacks formed by the HTC component iPP1, up to reach a good fit of experimental data of Young modulus. In Figure 6A, the values of Young modulus of our blends have been fitted quite well by the eq 3 in the whole range of composition (curve b). In this model, the values of p in the eq 3 decrease with the blend composition ϕ, according to the eq 4, and have been calculated for $\phi_{max} = 0.4$ using the eq 4 (symbols of Figure 6A′) and modeled with a sigmoid continuous function (curve a′ of Figure 6A′). Therefore, by using the concept of phase continuity and the results of ref 15, the experimental values of Young modulus of the blends iPP1/iPP2 blends in the whole range of composition may be fitted by eq 3 with practically no adjustable parameters. The gradual loss of phase continuity of the two components with increasing iPP2 content, for blends with $\phi > 0.4$, in turn, explains the fact that blends of nearly equimolar content of the two components show mechanical properties at low deformations intermediate between those of the *isostress* and *isostrain* models, and that the lower bound isostress behavior is already reached for blends with iPP2 content of 70 wt %.

The values of elastic recovery after breaking of the blends, reported in Figure 6D, clearly indicate that the blends iPP1/iPP2 with content of iPP2 higher than 50 wt % present significant elastomeric properties. It is also apparent from Figure 6D that the development of elastomeric properties in the blends with increasing concentration of the component iPP2 is "faster" than that observed in stereodefective iPP samples with increasing concentration of *rr* stereodefects.[11a,12]

It is worth noting that the gradual change of properties occurring in the blends iPP1/iPP2 with increasing the concentration of the low stereoregular component iPP2 from the properties of stiff plastic materials to the properties of elastomeric materials with high strength (Figure 6, full symbols), is parallel to the change of properties observed in the case of metallocene-made stereodefective iPP samples with increasing the concentration of *rr* stereodefects (Figure 6, open symbols). This analogy suggests defining for the blends iPP1/iPP2 the "*average degree of stereoregularity*", as the concentration of *rr* triads of the equivalent single component system ([*rr*(eq)]), as a unique parameter that well addresses the properties of the blends. Blends with high values of *average degree of stereoregularity* behave as stiff materials, blends with low values of *average degree of stereoregularity* become more flexible up to approach elastomeric properties.

In order to compare the elastomeric properties of samples stretched at different strains, the percentage of deformation which is recovered (R) have been evaluated as $R = 100 \times [(L_f - L_r)/[(L_f - L_0)]$, where L_0 and L_f are the initial and final lengths of the film stretched up to the deformation ε and L_r is the length of the relaxed sample after removing the tension. These values are reported in Figure 7 as a function of the blend composition. It is apparent from Figure 7 that the blends iPP1/iPP2 with content of the stereoirregular component iPP2 higher than 50 wt % show similar values of recovered strain at any deformation and after breaking indicating good elastomeric behavior regardless of the maximum elongation at which the sample is stretched. The elastomeric properties of the material increases with increasing the content of the stereoirregular component iPP2 and it is basically associated with the gradual decrease of crystallinity (Figure 2).

In the case of the blends iPP1/iPP2 with content of iPP2 higher than 30 wt %, the elastomeric properties have been studied also in oriented stress-relaxed fibers, prepared by stretching compression-molded films of initial length L_0 up to $\varepsilon = 250\%$ ($L_f = 3.5L_0$) and $\varepsilon = 500\%$ ($L_f = 6L_0$) and then removing the tension allowing complete relaxation of the specimens to the length L_r. The mechanical cycles of stretching and relaxation at room temperature of fibers of the blends iPP1/iPP2 and of the stereoirregular component iPP2, stress-relaxed from $\varepsilon = 250\%$ and $\varepsilon = 500\%$, are reported in Figure 8. In these hysteresis cycles stress-relaxed fibers of iPP2 (Figure 8A) and of blends iPP1/iPP2 (Figure 8B−D) of initial length L_r are stretched up to the final lengths $L_f = 3.5L_0$ or $L_f = 6L_0$ and then relaxed at controlled rate. For each sample at least four successive hysteresis cycles have been recorded, each cycle has been performed 10 min after the end of the previous cycle. After each cycle the values of the tension set and the percentage of dissipated energy have been measured and reported in Table 3.

The data of Figure 8 and Table 3 indicate that fibers of the blends iPP1/iPP2 with content of iPP2 higher than 50 wt % display good elastomeric properties, similar to that of the neat component iPP2. Regardless of the blend composition and of the maximum strain achieved during the preparation of the fibers, the values of tension set decrease after the first cycle and become zero after the second cycle (Table 3), the hysteresis curves successive to the second one being coincident, indicating a perfect elastic recovery. The values of the percentage of dissipated energy, instead, depend on the blend composition and increase with increasing the content of the stereoregular component iPP1, that is with increasing the degree of crystallinity (Table 3 and Figure 2). For instance, the sample iPP1−50/iPP2−50 with crystallinity of 56% presents a good elastomeric behavior with total elastic recovery ($t_s = 0$, after the first hysteresis cycle), but the range of elastic deformation is very small and is associated with a significant loss of mechanical energy (Figure 8D and Table 3).

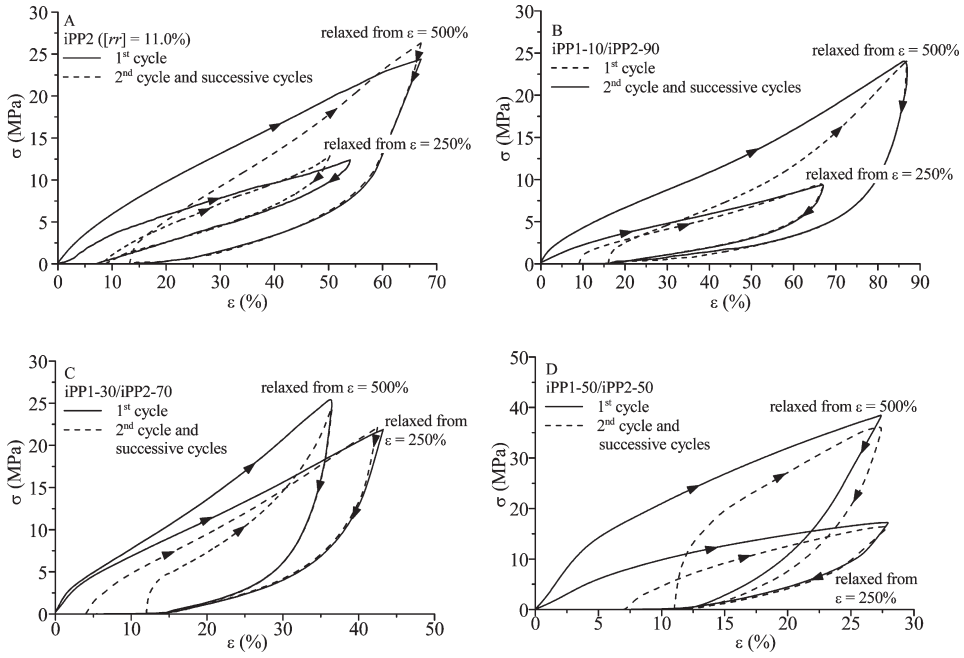

Figure 8. Stress−strain hysteresis cycles, composed of stretching and relaxation steps according to the directions of arrows, of fibers stress-relaxed from ε = 500% and ε = 250% of the sample iPP2 (A) and of the blends iPP1−10/iPP2−90 (B), iPP1−30/iPP2−70 (C), and iPP1−50/iPP2−50 (D). For each sample the first hysteresis cycle (solid lines) and the second cycle coincident to successive three cycles (dashed lines) are reported.

Table 3. Values of Tension Set (t_s) and Percentage of Dissipated Energy (W_{diss}) Measured in the Hysteresis Cycles of Figure 7 of Stress-Relaxed Fibers of the Neat Component iPP2 and the Blends iPP1/iPP2 with Content of iPP2 Higher than 30 wt %

sample	t_s (%) 1st cycle	t_s (%) 2nd cycle	t_s (%) 3th, 4th cycles	W_{diss} (%) 1st cycle	W_{diss} (%) 2nd -4th cycle
iPP2, ([rr] = 11.0%) ε = 250%	7 ± 4	2 ± 1	0	38	29
iPP1−10/iPP2−90 ε = 250%	9 ± 5	1.0 ± 0.5	1.0 ± 0.5	64	56
iPP1−30/iPP2−70 ε = 250%	4 ± 2	3 ± 1	0	76	60
iPP1−50/iPP2−50 ε = 250%	7 ± 1	2 ± 1	0	79	80
iPP2 ([rr] = 11.0%) ε = 500%	13 ± 4	0	0	68	40
iPP1−10/iPP2−90 ε = 500%	16 ± 2	1.0 ± 0.5	0	75	65
iPP1−30/iPP2−70 ε = 500%	12 ± 2	2 ± 1	0	76	60
iPP1−50/iPP2−50 ε = 500%	11 ± 1	0	0	77	75

The remarkable values of tensile strength (Figures 5 and 6B) associated with low values of plastic residual deformation (Figures 7, 8 and Table 3) of the blends iPP1/iPP2 having content of the stereoirregular component iPP2 higher than 30 wt %, are probably related to the high values of crystallinity of the samples (x_c = 40−56%) and to the occurrence of structural transformations during deformation.

The X-ray diffraction patterns of fibers of the samples iPP1−90/iPP2−10, iPP1−50/iPP2−50, and iPP1−10/iPP2−90 stretched at different values of strain, keeping the fibers under tension and after removing the tension, are reported in Figure 9, as an example. In the case of the blends with high content of the highly isotactic component iPP1, crystals of α form initially present in the compression-molded unstretched film (curve b of Figure 1B) are still not well oriented in the fiber stretched at 100% deformation (Figure 9A). These crystals gradually transform into the mesomorphic form by stretching (Figure 9B) and at 400% deformation fibers in pure mesomorphic form are obtained (Figure 9C). Formation of mesomorphic form is indicated by the progressive broadening along the equator of the Debye−Scherrer rings relative to 110, 040, and 130 reflections of α form, which, with increasing the deformation, merge into a single halo spanning the 2θ range of 14−18° and become well polarized on the equator in the diffraction pattern of Figure 9C. Crystals of α form that undergo plastic deformation and achieve orientation rapidly transform into the mesomorphic form (Figure 9A−C) and no oriented crystals of α form are observed in the patterns of Figure 9A−C.

The complete transformation of α or γ forms into the mesomorphic form by stretching at room temperature has also been observed in stereodefective iPP samples having concentration of *rr* stereodefects higher than 3−4 mol %.[11,12] It has been suggested that the easy formation of the mesomorphic form accounts for the high flexibility and ductility of these iPP samples.[12] In fact, in these samples defective crystals of γ form are easily deformed and destroyed by mechanical melting followed by recrystallization into the mesomorphic form.[29] The formation of mesomorphic aggregates, in turn, facilitates further stretching up to very high values of strain resulting in high flexibility.[12] In the case of the highly stereoregular samples

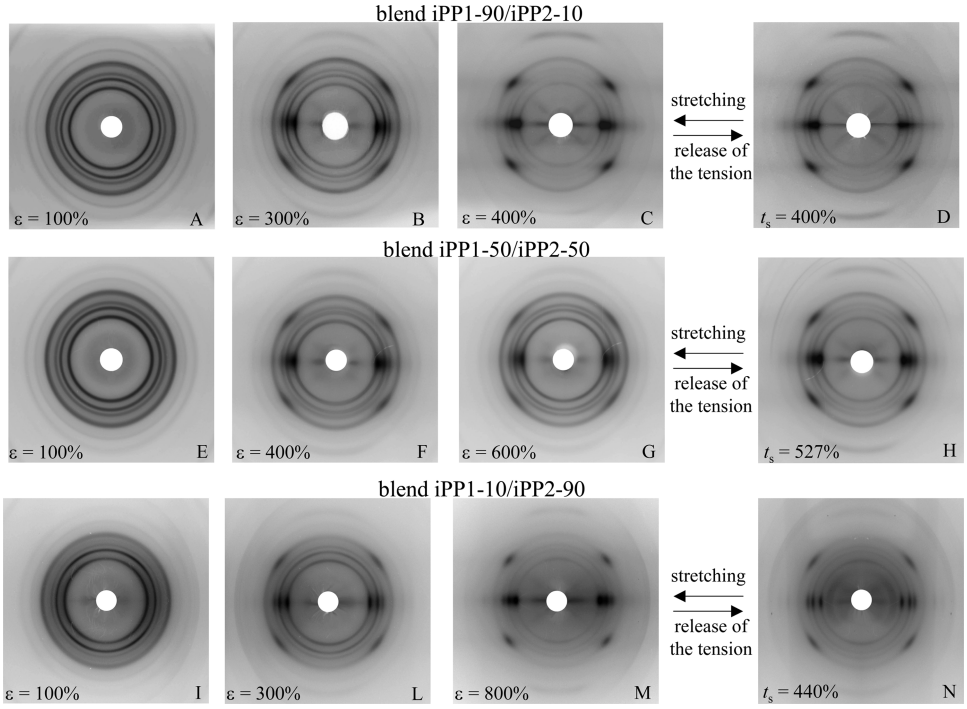

Figure 9. X-ray diffraction patterns of fibers of the samples iPP1/10-iPP2−90 (A−D), iPP1−50/iPP2−50 (E−H), and iPP1−10/iPP2−90 (I−N) stretched at different values of strain ε, keeping the fibers under tension and after removing the tension. The values of tension set (t_s) measured after relaxation of specimens are also indicated.

(with *rr* content lower than 2−3 mol %), as the sample iPP1 ([*rr*] = 0.49%), only a small fraction of crystals of α form present initially in the compression-molded film transforms into the mesomorphic form.[12] Most of the crystals of α form has high resistance to the plastic deformation and does not transform into the mesomorphic form before breaking of the sample (ε = 200−300%, Figure 5).[12] This results in highly stiff and less ductile materials.[11,12] It is worth noting that the stress-induced phase transition of α and/or γ forms into the mesomorphic form of iPP has been already observed not only in the case of metallocene-made stereodefective iPP samples having concentration of *rr* stereodefects higher than 3−4 mol %,[11,12] but also in the case of stretching at room temperature of iPP samples prepared with Ziegler−Natta catalysts.[29] As shown in ref[29] studies performed by use of small angle and wide-angle X-ray diffraction have indicated that there was no lamellar structure in the mesomorphic form of the iPP fibers. It has been suggested that the formation of the mesophase is through the destruction of the lamellar crystalline phase, probably by pulling chains out from crystals, and the dominant constituent of the mesomorphic form may be oriented bundles of helical chains.

In the case of the blends iPP1/iPP2, the addition of even small amounts of the stereoirregular component iPP2 allows achieving high deformations without breaking (Figure 5). The increase of ductility, in turn, allows reaching deformations high enough before breaking so that transformation of pre-existing crystals of α form of the highly stereoregular component iPP1 (Figure 9A) into the mesomorphic form (Figure 9C) may occur. We argue that the increase of ductility is associated with the good level of miscibility iPP1 and iPP2 in the melt and in the amorphous state, the formation of mixed lamellar stacks of the two components where the lamellae of the LCT component iPP2 are entirely included inside the lamellar stacks of the major component, and the consequent buildup of a continuous network.[15] More precisely, the miscibility of iPP1 and iPP2 chains in the intralamellar amorphous regions creates phase continuity of the two components even at high deformations and an effective mechanism able to transmit the stress all over the sample. We presume that at these high deformations, when the mechanical energy adsorbed by the crystalline phase becomes high enough, the formation of the mesomorphic form occurs probably via the pulling out of the chains from pre-existing lamellae and successive reorganization of the chains in the mesomorphic aggregates.[29] Therefore, resorting to the concept of "*average tacticity*", contrary to the pure component iPP1, blends with low iPP2 content show high ductility and stress-induced phase transitions similar to those observed in the case of iPP homopolymer samples with *rr* concentration close to the value of the "*average tacticity*" of blend.

For the blend iPP1−90/iPP2−10 the mesomorphic form obtained by stretching at high deformation remains stable upon removing the tension (Figure 9D) and, correspondingly, the material does not show elastomeric behavior. A similar behavior has been observed in blends with higher concentration of the stereoirregular component iPP2.

In the blend iPP1−50/iPP2−50 crystals of α form present in the compression-molded film (profile d of Figure 1B) transforms into the mesomorphic form by stretching (Figure 9E-G). The decrease of crystallinity (profile d of Figures 1B and Figure 2) and of the "*average tacticity*", due to the increase of the content of the stereoirregular component iPP2, reduces the value of critical stress necessary for inducing plastic deformation so that the transition into the mesomorphic form occurs at deformations (ε = 600−700%, Figure 9G) higher than the deformation necessary to promote formation of the mesophase in the blends with lower content of iPP2. However, even at the maximum

dx.doi.org/10.1021/ma201420f |*Macromolecules* 2011, 44, 6026–6038

achievable deformations prior to breaking, along with the broad halo in the range $2\theta = 14-18°$ of the mesomorphic form, reflections of non oriented crystals of α form are still present in the diffraction pattern of Figure 9G. This indicates that at high values of strain only a portion of the crystals initially present in the sample experiences the mechanical stress field and transforms into well oriented aggregates of chains of the mesomorphic form. A portion of crystals of α form, instead, remains unoriented and does not experience any polymorphic transformation in the fibers of the blend iPP1−50/iPP2−50. The composite diffraction pattern of this blend at high deformations (Figure 9G) reflects the fact that the chains of iPP1 and iPP2 components form two interpenetrating networks at 50 wt % composition. According to SAXS data analysis of ref 15 different families of mixed lamellar stacks are formed in this blend. For the network dominated by the chains of the component iPP1 the lamellar crystals of iPP1 prevail, whereas for the network dominated by the component iPP2, the lamellar crystals of iPP2 become prevalent. Complete transformation into the mesomorphic form probably occurs only for the crystals of the component iPP1 embedded in the network dominated by chains of the highly stereoregular component, since only these crystals may easily experience the mechanical stress field. The portion of iPP1 crystals embedded in the network dominated by the chain of the low stereoregular component iPP2, instead, are less affected by the mechanical stress field, probably also due to the highly compliant nature of the tie chains connecting the crystals, associated with the low value of the "*average tacticity*" at local scale. As a consequence, the deformation needed to transmit an effective stress field also to these crystals, able to promote their transformation into the mesomorphic form, would be so high that the sample breaks prior to the occurrence of mechanical melting.

Also for the blend iPP1−50/iPP2−50 the mesomorphic form obtained by stretching remains stable upon releasing the tension (Figure 9H) and only poor elastic recovery is observed (Figure 8D).

Finally, the blends iPP1/iPP2 rich in the low stereoregular component iPP2 present high flexibility, strain hardening at high deformation and elastomeric properties (Figure 5 and 8B,C). The structural transformations occurring during stretching of the blend iPP1−10/iPP2−90 are shown in Figure 9I−N. Highly defective crystals of α/γ disordered modifications present in the compression-molded film (profile f of Figure 1B), transform by stretching into the α form (Figure 9L) and, then, only in part into the mesomorphic form at higher deformation close to the breaking (Figure 9M). Contrary to the blends iPP1/iPP2 with higher content of iPP1, in these samples the mesomorphic form obtained by stretching at high deformation is stable only in the stretched fibers and transforms into the α form when the tension is removed (Figure 9N). This transition is reversible upon successive stretching and relaxation (Figure 9M,N). Correspondingly, fibers of the blend iPP1−10/iPP2−90 show elastomeric properties (Figure 8B).

This behavior is similar to that of the stereodefective sample iPP2 and of iPP samples with content of *rr* stereodefects higher than 6−7 mol %.[11,12] In stereodefective iPPs and in blend iPP1/iPP2 with content of iPP2 higher than 50 wt % the elastomeric properties are associated with the reversible structural transition between the α form and the mesomorphic form. This transition provides an enthalpic contribution to the elasticity,[12] and is responsible for the outstanding properties of high-strength elastomers of fibers of the blends iPP1/iPP2 with content of iPP2 higher than 50 wt % (Figures 5 and 8).

In these elastomeric materials the values of Young's modulus can be regulated by changing the concentration of the stiff component iPP1 (Figure 6A), whereas the strong strain hardening occurring at high deformations, which is related to the structural transformations and orientation of the elastomeric network, produces value of strength even higher than that observed in more crystalline and stiff blends containing high concentration of the more crystalline component iPP1.

CONCLUSIONS

The structure and mechanical properties of blends of iPP samples of different stereoregularity (a highly isotactic and crystalline sample iPP1 and a poorly isotactic and elastomeric sample iPP2), prepared with two different metallocene catalysts, have been analyzed. These blends form crystalline lamellar stacks with a high degree of inclusion of both components in the same stack.

Thermal analysis of blends reveals separate melting and crystallization of the two components at temperatures close to those of neat components regardless of composition and thermal history of the samples. The analysis of the mechanical properties shows that the tensile properties of the blends iPP1/iPP2 depend on the composition, ranging from the properties of the highly stereoregular and stiff component iPP1 to those of the stereoirregular and elastomeric component iPP2. The values of Young's modulus gradually decrease and the ductility and flexibility increase with increasing the concentration of the stereoirregular component iPP2, in agreement with the decrease of crystallinity. Moreover, blends with content of iPP2 higher than 50 wt % show good elastomeric properties associated with a reversible structural transition between the mesomorphic form obtained by stretching and the crystalline α form obtained by releasing of the tension.

The change of mechanical behavior of the blends iPP1/iPP2 of different composition reflects the peculiar morphology of these blends at nanometer length scale and, in particular, the formation of a continuous network guaranteed by the miscibility of the components in the melt and in the amorphous phase, in which the well interlocked crystalline lamellae of iPP1 and iPP2 components form junctions of nanometer size. Moreover, it has been shown that the continuous change of the tensile properties of the blends iPP1/iPP2 with the composition is similar to the change of mechanical properties observed in the case of metallocene-made stereodefective iPP samples characterized by different concentrations of *rr* defects. This behavior suggests that for these blends the concept of "*average degree of stereoregularity*" *rr*(eq) can be used to uniquely address their properties. This parameter, indeed, formally identifies for each blend composition the concentration of *rr* triads of an equivalent single component system obtained as if the concentration of *rr* triads defects of iPP1 and iPP2 was uniformly distributed over all the chains. Several properties of our blends are similar to those of an equivalent single component system with degree of stereoregularity numerically coincident with *rr*(eq). In particular the concept of "*average degree of stereoregularity*" explains (i) the neat increase of ductility of iPP1 already by addition of small amounts of iPP2; (ii) for the iPP1 rich blends, the increase of critical value of strain able to promote full transformation of the initial α form into the mesomorphic form; (iii) the appearance of non trivial elastomeric

properties in iPP2 rich blends already for blends with iPP2 content higher than 50 wt %; (iv) the overall change of properties (i.e., crystallinity, Young's modulus, elasticity, stress at break) with composition.

From practical standpoint, we have shown that addition of the low stereoregular sample iPP2 to the highly stereoregular iPP1 provides a facile route for tailoring material properties, obtaining materials with mechanical properties of highly stiff plastomers, high flexibility, or high-strength elastomers by simple change of the blend composition. Since a similar range of properties can also be obtained by tailoring the concentration of *rr* stereodefects, using different metallocene catalysts, the advantage of preparing binary blends of two iPP samples having very different concentration of *rr* defects for obtaining the same properties is that only two different catalysts must be used.

■ ASSOCIATED CONTENT

Supporting Information. Stereodefective isotactic polypropylenes as reference samples, including structures and data, additional DSC data, and a thermal analysis. This material is available free of charge via the Internet at http://pubs.acs.org.

■ AUTHOR INFORMATION

Corresponding Author

*(F.A.) Telephone: ++39 081 674341. Fax: ++39 081 674090. E-mail: finizia.auriemma@unina.it. (O.R.d.B.) Telephone: ++39 081 674448. Fax: ++39 081 674090. E-mail: odda.ruizdeballesteros@unina.it.

■ ACKNOWLEDGMENT

Financial support from Basell Poliolefine Italia S.r.l., "a LyondellBasell company" (Ferrara) and from INSTM (PRISMA Project 2007) are gratefully acknowledged. Dr. Luigi Resconi of Borealis Polyolefine GmbH, Linz (Austria) is also acknowledged for useful discussions.

■ REFERENCES

(1) (a) Nwabunma, D.; Kyu, T. *Polyolefin Blends*; Wiley-Interscience: Hoboken, NJ, 2008. (b) Shiomura, T.; Uchikawa, N.; Asanuma, T.; Sugimoto, R.; Fujio, I.; Kimura, S.; Harima, S.; Akiyama, M.; Kohno, M.; Inoue, N. In *Metallocene Based Polyolefins: Preparation, Properties and Technology*; Scheirs, J., Kaminsky, W., Eds.; John Wiley & Sons: Chichester, England, 2000; Vol. 1, pp 437−465.

(2) (a) Phillips, R. A. *J. Polym. Sci., Part B: Polym. Phys.* **2000**, *38*, 1947. (b) Wang, Z.-G.; Phillips, R. A.; Hsiao, B. S. *J. Polym. Sci., Part B: Polym. Phys.* **2000**, *38*, 2580. (c) Mayer, R.-D.; Thomann, R.; Kressler, J.; Mulhaupt, R.; Rudolf, B. *J. Polym. Sci., Part B: Polym. Phys.* **1997**, *35*, 1135. (d) Silvestri, R.; Sgarzi, P. *Polymer* **1998**, *39*, 5871. (e) Chien, J. C. W.; Iwamoto, Y.; Rausch, M. D.; Wedler, W.; Winter, H. H. *Macromolecules* **1997**, *30*, 3447.

(3) Woo, E. M.; Cheng, K. Y.; Chen, Y.-F.; Su, C. C. *Polymer* **2007**, *48*, 5753.

(4) Newman, S.; Cox, W. P. *J. Po1ym. Sci.* **1960**, *46*, 29.

(5) (a) Liu, J.; Junnickel, B. J. *J. Polym. Sci., Polym. Phys. Ed.* **2007**, *45*, 1917. (b) Schultz, J. M. *Front. Chem. China* **2010**, *5*, 262.

(6) (a) Groeninckx, G.; Vanneste, M.; Everaert, V. In *Polymer Blends Handbook*; Utracki, L.A., Ed.; Kluwer Academic Publishers: Amsterdam, 2003; p 203. (b) Paul, D. R.; Bucknall, C. B. In *Polymer Blends*; Wiley-Interscience: New York, 1999; Vol. 2.

(7) Mandelkern, L. In *Crystallization of Polymers*; New York: Cambridge University Press: Cambridge, U.K., 2002; Vol. 1.

(8) Resconi, L.; Cavallo, L.; Fait, A.; Piemontesi, F. *Chem. Rev.* **2000**, *100*, 1253.

(9) Resconi, L. In *Synthesis of atactic polypropylene using metallocene catalysts*; Kaminsky, W.; Scheirs, J., Eds.; Wiley: New York, 1999; Vol. 1, p 467; Balboni, D.; Moscardi, G.; Baruzzi, G.; Braga, V.; Camurati, I.; Piemontesi, F.; Resconi, L.; Nifant'ev, I.; Venditto, V.; Antinucci, S. *Macromol. Chem. Phys.* **2001**, *202*, 2010–2028.

(10) Chum, P. S.; Swogger, K. W. *Prog. Polym. Sci.* **2008**, *33*, 797.

(11) (a) De Rosa, C.; Auriemma, F.; Di Capua, A.; Resconi, L.; Guidotti, S.; Camurati, I.; Nifant'ev, I. E.; Laishevtsev, I. P. *J. Am. Chem. Soc.* **2004**, *126*, 17040. (b) Resconi, L.; Balboni, D.; Baruzzi, G.; Fiori, C.; Guidotti, S.; Mercandelli, P.; Sironi, A. *Organometallics* **2000**, *19*, 420. (c) Resconi, L.; Guidotti, S.; Camurati, I.; Frabetti, R.; Focante, F.; Nifant'ev, I. E.; Laishevtsev, I. P. *Macromol. Chem. Phys.* **2005**, *206*, 1405.

(12) (a) De Rosa, C.; Auriemma, F. *J. Am. Chem. Soc.* **2006**, *128*, 11024. (b) De Rosa, C.; Auriemma, F. *Lect. Notes Phys.* **2007**, *714*, 345. (c) De Rosa, C.; Auriemma, F.; De Lucia, G.; Resconi, L. *Polymer* **2005**, *46*, 9461.

(13) (a) De Rosa, C.; Auriemma, F.; Resconi, L. *Macromolecules* **2005**, *38*, 10080. (b) De Rosa, C.; Auriemma, F.; Paolillo, M.; Resconi, L.; Camurati, I. *Macromolecules* **2005**, *38*, 9143.

(14) A similar approach has been pursued earlier by blending a highly isotactic PP produced with a highly isospecific Ziegler−Natta catalyst and different polypropylenes of lower isotacticity from metallocene catalysts; see, for example:Resconi, L.; Ferraro, A.; Baruzzi, G. *Thermoplastic compositions of isotactic propylene polymers and flexible propylene polymers having reduced isotacticity and a process for the preparation thereof.* Int. Pat. Appl. WO 2001/070878 to Basell Technology Company.

(15) Auriemma, F.; Ruiz de Ballesteros, O.; De Rosa, C. *Macromolecules* **2010**, *43*, 9787.

(16) Hotta, A.; Cochran, E.; Ruokolainen, J.; Khanna, V.; Fredrickson, G. H.; Kramer, E. J.; Shin, Y.-W.; Shimizu, F.; Cherian, A. E.; Hustad, P. D.; Rose, G. M.; Coates, G. W. *Proc. Natl. Acad. Sci. U.S.A.* **2006**, *103*, 15327–15332.

(17) Moraglio, G.; Gianotti, G.; Bonicelli, U. *Eur. Polym. J.* **1973**, *9*, 693.

(18) Alamo, R. G.; Kim, M.; Galante, M. J.; Isasi, J. R.; Mandelkern, L. *Macromolecules* **1999**, *32*, 4050.

(19) (a) VanderHart, D. L.; Alamo, R. G.; Nyden, M. R.; Kim, M. H.; Mandelkern, L. *Macromolecules* **2000**, *33*, 6078. (b) Alamo, R. G.; VanderHart, D. L.; Nyden, M. R.; Mandelkern, L. *Macromolecules* **2000**, *33*, 6094.

(20) Thomann, R.; Wang, C.; Kressler, J.; Mülhaupt, R. *Macromolecules* **1996**, *29*, 8425.

(21) (a) De Rosa, C.; Auriemma, F.; Circelli, T.; Waymouth, R. M. *Macromolecules* **2002**, *35*, 3622. (b) Auriemma, F.; De Rosa, C. *Macromolecules* **2002**, *35*, 9057.

(22) (a) De Rosa, C.; Auriemma, F.; Ruiz de Ballesteros, O.; Resconi, L.; Camurati, I. *Macromolecules* **2007**, *40*, 6600. (b) De Rosa, C.; Auriemma, F.; Ruiz de Ballesteros, O.; Resconi, L.; Camurati, I. *Chem. Mater.* **2007**, *19*, 5122.

(23) Natta, G.; Corradini, P. *Nuovo Cimento Suppl.* **1960**, *15*, 40.

(24) (a) Brückner, S.; Meille, S. V. *Nature* **1989**, *340*, 455. (b) Meille, S. V.; Brückner, S.; Porzio, W. *Macromolecules* **1990**, *23*, 4114.

(25) (a) Auriemma, F.; De Rosa, C.; Boscato, T.; Corradini, P. *Macromolecules* **2001**, *34*, 4815. (b) De Rosa, C.; Auriemma, F.; Perretta, C. *Macromolecules* **2004**, *37*, 6843.

(26) (a) Manson, J. A.; Sperling, L. H. In *Polymer Blends and Composites*; Heyden: London, 1976; p 67; (b) Takayanagi, M.; Harima, H.; Iwata, Y. *Mem. Fac. Eng. Kyushi Univ.* **1963**, *23*, 1. (c) McCullough, R. L. In *Treatise on Materials Science and Technology*; Schultz, J. M., Ed.; Academic Press: San Diego, CA, 1977; Vol. 10B, p 453.

(27) Kolarik, J. *Poly. Eng. Sci.* **1996**, *36*, 2518.

(28) The volume fraction of iPP1 and iPP2 constituents in the blends may be assumed to a good approximation nearly coincident with the mass fraction.

(29) Ran, S.; Zong, X.; Fang, D.; Hsiao, B. S.; Chu, B.; Phillips, R. A. *Macromolecules* **2001**, *34*, 2569.